BIOMASS PYROLYSIS: THERMODYNAMIC PARAMETERS REVIEW AND DETERMINATION THROUGH TGA

Joanna D'Antoni[1,2]*, Amine Ben Abdelwahed[1,2], Cécile Gaborieau[1], Audrey Duphil[1], Wahbi Jomaa[1], Jean Lachaud[1]

[1]University of Bordeaux - Institute of Mechanics and Engineering, Talence, France
[2]Arts et Métiers Institute of Technology - Institute of Mechanics and Engineering, Talence, France
*joanna.dantoni@u-bordeaux.fr

ABSTRACT

In this work, the focus is set on the development of thermochemistry models for hardwood (HW) pellets pyrolysis reaction at heating rates ranging from 10 to 60 K/min. Thermogravimetric Analysis (TGA) coupled with Differential Scanning Calorimetry (DSC) was used to determine the following parameters: Activation Energy (Ea), pre-exponential factor (A), order of reaction (n) and mass loss fractions of pseudo components (F_i). These parameters have been determined thanks to an optimization approach (Torres-Herrador et al. 2020) as well as isoconversional methods. Activation energies were determined for drying of water (30-35 kJ/mol), and for the pyrolysis of pseudo components hemicellulose (155-160 kJ/mol), cellulose (170-185 kJ/mol) and lignins (220-230 kJ/mol). Combined TGA/DSC results highlight the correlation between the degradation of the different compounds (cellulose, hemicellulose, lignins) and the heat flux released. The results were then juxtaposed with existing literature data using a comprehensive comparison graph. Comparison between the determination techniques and the associated results in literature was performed to determine their impact on the parameters found.

1 INTRODUCTION

Pyrolysis is a thermal process in which biomass, such as wood, agricultural waste, or plants, is decomposed in the absence of oxygen to produce pyrolysis gases, tars, and char. These byproducts offer various potential uses: heavy gases and tars contain valuable bio-hydrocarbon molecules which can be used as biofuels or in other industrial applications. Lighter gases can be converted into synthesis gas or biogas for heat, electricity or fuel. Biochar can be used in agriculture to improve soil fertility and water retention, while also serving as a filter in wastewater treatment (Hu and Gholizadeh 2019). Besides, char can further react with steam or air through gasification, producing either hydrogen or methane.

Thermogravimetric analysis (TGA), particularly the derivative thermogravimetric (DTG) curve, is frequently employed for the study of thermochemical processes involving biomass (Ranzi et al. 2008). This technique enables the identification of distinct stages in biomass pyrolysis by measuring the mass loss in regard to the temperature, which allows to retrieve the thermodynamic parameters of the reaction. Pyrolysis parameters are frequently determined with a one-component approach, generally through model-free fitting and isoconversional methods (Dhaundiyal, Mohammad, and Laszlo 2019; Mishra and Mohanty 2018; Yan et al. 2020). However, biomass pyrolysis should be modeled as a multi-component process to accurately reproduce experimental data (Di Blasi 2008). Detailed models have been developed, grouping similar components and lumping some reactions, allowing a model capable of satisfactorily describing a variety of biomass pyrolysis (Ranzi et al. 2008). These models are detailed but pragmatic and show reasonable agreement at the process level for various conditions (Blondeau and Jeanmart 2012; Corbetta et al. 2014). This approach is limited by the extensive experimental work required to develop models for new resources, as each compound needs to be characterized separately. A well-accepted approach for fast yet effective investigation is to describe biomass pyrolysis by considering it as the sum of its primary pseudo-components degradation reactions: water, hemicellulose, cellulose, and lignins (Shafizadeh and Chin 1977). This work suggests the use of coupled TGA/DSC, as well as Multi-objective Optimization method (MO) in order to determine a wide set of thermodynamic parameters for each pseudo component, with a limited set of experiments: Activation

https://doi.org/10.52202/077185-0175

energies (Ea), pre-exponential factors (A) order of reactions (n) and mass loss fractions (F_i) were determined by an original parameter identification tool using optimization (Torres-Herrador et al. 2020). Ea and $\log(A)$ values were then calculated for each pseudo component by isoconversional method, after performing Asymmetric Double Sigmoidal (Asym2sig) function deconvolution (Chen et al. 2017; Mumbach et al. 2022; Romero Millán, Sierra Vargas, and Nzihou 2017).
The impact of the determination technique on the parameters obtained will be studied in order to assess the reliability of results found in literature and make more informed comparison.
In a first part, the kinetic parameters will be determined through optimization, followed by isoconversional method using results from TGA. The DSC data will then be analyzed and correlated with TGA to validate the obtained results. Finally, a literature review will be provided to compare the obtained kinetic parameters with those from literature.

2 MATERIALS AND METHOD

2.1 Biomass sample

The biomass samples used in this work are pellets of hardwood (HW) sawdust. The proportion of each pseudo-component vary depending on the type of material considered, but values are usually in the range of 24-40% for hemicellulose, 40-55% for cellulose and 18-25% for the lignins (Sun and Cheng 2002). Chemical analysis of hardwood sawdust pellets has been conducted several times in literature, in order to find the material elemental composition (Bandara et al. 2021; Janković et al. 2018; Mishra and Mohanty 2018; Saeed et al. 2019). **Table 1** showcases the range obtained from the literature.

Table 1: Chemical composition of hardwood pellets

	Values
C [wt.%]	49.4 – 50.9
H [wt.%]	5.9 – 6.8
O [wt.%]	41.8 – 43.6
N [wt.%]	0.03 – 0.6

TGA measurements have allowed to measure the moisture content (7.5-8.3 wt.%) and the volatile content (80.5-84.5 wt.%) of the material. Combustion reaction gives the ash content (1-1.8 %), which allows to retrieve the Fixed Carbon content (13.7-18.5 wt%).

2.2 Combined TGA/DSC

The experiments were carried out on a TGA/DSC 3+ from Mettler. Within the chamber, a platform serves as the placement area for both the sample and an empty crucible used as a reference. This platform is connected to a precision balance, continuously measuring the sample's mass. Additionally, thermocouples are positioned beneath each crucible. By analyzing the temperature differences, the DSC provides a precise measurement of the heat absorbed or released during a reaction. Platinum crucibles were employed to optimize heat transfer between the thermocouples and crucibles. Lids were intentionally omitted from the crucibles to prevent tar deposition.
The system is swept by Argon at 50 ml/min to evacuate the pyrolysis gases and avoid any oxygen return. The wood pellets were crushed into powder to improve heat transfers inside the material. Samples of 24 mg (± 0.5 mg) were pyrolyzed at a temperature varying between 30 and 700°C, at four controlled heating rates: 10, 20, 30 and 60 K/min.

2.3 TGA curves analysis

The mass loss curves obtained by TGA were differentiated in regard to the temperature, allowing to obtain peaks of mass loss. These derivatives, called DTG, are represented in absolute value for clarity. Two methods were employed to determine parameters of Arrhenius' law, presented in 2.5 and 2.6. Di Blasi's studies demonstrated the existence of compensation effects among parameters during the identification of kinetic parameters from TGA experiments. To address this issue, conducting parameter identification with multiple datasets obtained at varying heating rates is recommended. This approach helps constrain the problem, resulting in a singular and definitive solution (Di Blasi 2008).

https://doi.org/10.52202/077185-0175

2.4 Arrhenius law

Arrhenius law is commonly used to represent the pyrolysis reaction and is given by:

$$\frac{d\chi}{dt} = A(1-\chi)^n \exp\left(-\frac{Ea}{RT(t)}\right) \quad (1)$$

Where χ describes the advancement of the reaction in regard to the temperature T evolution in time (before the reaction, $\chi = 0$ and $\chi = 1$ when the pyrolysis is complete), Ea is the Activation Energy, A is the preexponential factor, n the order of reaction and R the ideal gas constant. Theses parameters are used to model one pyrolysis reaction. Modelling biomass pyrolysis as a single reaction usually fails to efficiently reproduce the complex material decomposition (Di Blasi 2008). This work employs a multi-component reaction, in which each component i is decomposed independently following its own Arrhenius law. The reaction can then be described as a sum of advancements, following the equation:

$$\frac{m(t)}{m_0} = 1 - \sum_{1}^{N} F_i . \chi_i(t) \quad (2)$$

The equation above, described by (Torres-Herrador et al. 2020), allows to retrieve the total material mass loss m thanks to the advancement χ_i and the mass loss fraction F_i of each component.

2.5 Fitting TGA Algorithm

In order to determine the Arrhenius parameters of the pyrolysis reaction, Torres-Herrador et al. 2020 developed a fitting algorithm (FiTGA) that identifies kinetics parameters by optimization.
FiTGA uses a two-step mechanism: first, a global yet imprecise solution is found through a global optimization algorithm (shuffled complex evolutionary and genetic algorithm). This solution is then refined by a gradient based method (nonlinear least-squares method) (Torres-Herrador et al. 2020).
Four reactions were considered for the decomposition of the biomass based on its three main components (cellulose, hemicellulose, and lignins), along with water.

2.6 Isoconversional methods

Model-free methods use the hypothesis of a simple reaction, during which the raw material is converted into volatiles and char (Mishra and Mohanty 2018). In this case, the conversion rate χ is defined as the total mass loss evolution varying in time between 0 and 1:

$$\chi(t) = \frac{m_0 - m(t)}{m_0 - m_f} \quad (3)$$

Introducing the heating rate $\beta = \frac{dT}{dt}$ in Eq. (1), the Arrhenius law can be written as:

$$\frac{d\chi}{dT} = \frac{A}{\beta} . (1-\chi)^n \exp\left(-\frac{Ea}{RT}\right) \quad (4)$$

By integration with respect to temperature, an integral function $g(\chi)$ can be obtained:

$$g(\chi) = \int_0^{\chi} \frac{d\chi}{(1-\chi)^n} = \int_{T_0}^{T} \frac{A}{\beta} \exp\left(-\frac{Ea}{RT}\right) dT \quad (5)$$

These methods follow the assumption that the order of reaction is constant and equal to 1.
In this work isoconversional Friedman, KAS and OFW models, which are widely applied for biomass combustion and pyrolysis kinetics, were used to determine activation energies for each different pseudo-component as described in **Table 2**. Left hand side of equations are plotted versus inverse absolute temperature times the ideal gas constant (-1/RT) to obtain the slope of the graph for estimation of activation energies at each conversion point χ.

https://doi.org/10.52202/077185-0175

Table 2: Applied equations of isoconversional models for kinetic study

Model	Model equation
Friedman	$\ln\left(\frac{d\chi}{dt}.\beta\right) = \ln\left(A.(1-\chi)^n\right) - \frac{E_a}{RT(t)}$
KAS	$\ln\left(\frac{\beta}{T^2}\right) = \ln\left(-\frac{A.E_a}{Rg(\chi)}\right) - \frac{E_a}{RT(t)}$
OFW	$\ln(\beta) = \ln\left(-\frac{A.E_a}{Rg(\chi)}\right) - 5.331 - 1.052\frac{E_a}{RT(t)}$

The pre-exponential factor can be calculated by Eq. (6) (ASTM D 698 1999; Xu and Chen 2013):

$$A = \beta.E_a.\exp\frac{E_a}{R.T_p}/(R.T_p^2) \tag{6}$$

Where T_p represents the DTG peak temperature.

2.7 Deconvolution

In order to find Ea for the different pseudo components, a deconvolution was performed to divide the total DTG curve into four asymmetrical gaussians, following Asymmetric Double Sigmoidal (Asym2sig) function (Chen et al. 2017; Mumbach et al. 2022).

$$\frac{d\chi}{dt} = \frac{\theta}{1+\exp\left(-\frac{T-T_p+\frac{w_1}{2}}{w_2}\right)}.\left(1-\frac{1}{1+\exp\left(-\frac{T-T_p-\frac{w_1}{2}}{w_3}\right)}\right) \tag{7}$$

Were θ represents the maximum amplitude of the curve, T_p the peak temperature, w_1 the curve width, w_2 and w_3 the offsets in the left and right direction.

These gaussians were generated in order to fit the FiTGA peaks in terms of placement, maximum height and surface. The peaks were then grouped by the corresponding stage, and isoconversional analysis was performed. The χ values for each stage were adjusted from 0 to 1 as each stage was analyzed as an independent reaction for each pseudo-component.

3 RESULTS AND DISCUSSION

3.1 Thermal degradation

The mass loss during the pellet pyrolysis process and its derivative (mass loss rate) are shown in **Figure 1** as a function of the sample temperature.

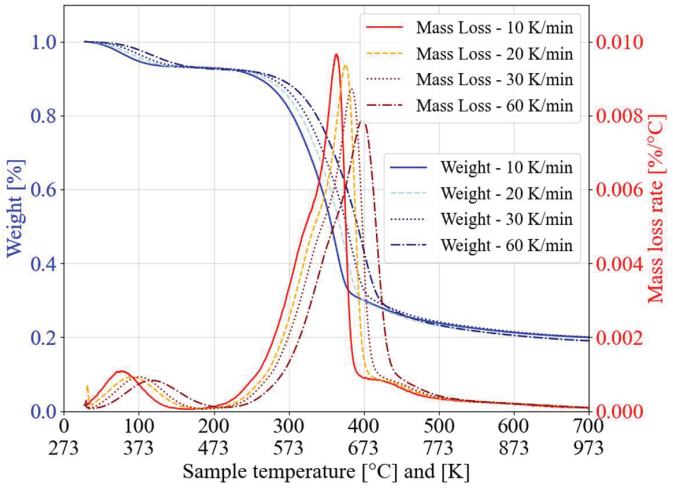

Figure 1: TGA (Mass loss) and DTG (Mass loss rate) results at different heating rates

https://doi.org/10.52202/077185-0175

Three zones can be observed in the degradation curves: A first one can be determined from 50 to 200°C, during which a small weight loss can be observed. This mass loss, appearing as small peaks centered around 100°C, corresponds to the water evaporation. The second zone, between 200 and 500°C corresponds to the pyrolysis reaction. Three peaks can be observed, corresponding to the hemicellulose (between 250 and 350 °C), cellulose (between 350 and 450 °C) and lignins (between 400 and 450°C) degradation. Those peaks overlap, a phenomenon accentuated with the increase of the heating rate. Indeed, the peaks move towards higher temperatures with the heating rate because the reduced reaction time leads to a less efficient thermal transfer to the biomass, with thermal hysteresis phenomena.
Finally, a passive pyrolysis stage can be observed in the range of 450–600 °C, during which the mass slowly decreases, as the last and more complex parts of the biomass decompose (Collard and Blin 2014). In those three steps, an average mass loss of 8 ± 0.5 wt%, 72 ± 2 wt% and 2 ± 0.5 wt% was observed.

3.2 Identification of Kinetic Parameters with FiTGA

FiTGA was used with a four-component scheme in order to identify the kinetic parameters. **Figure 2** depicts a comparison between the experimental DTG and the ones calculated by the optimization tool. FiTGA reproduced quite accurately the mass loss rate evolution at the four heating rates studied, but one can remark that the same parameters can not represent a large range of heating rates, as the extrema (10 and 60 K/min) are less accurately reproduced. Indeed, the use of parallel schemes in biomass does not allow to reproduce a wide range of heating rates (Park, Atreya, and Baum 2010).

The shadowed areas represent the decomposition of the pseudo-components: the peak of water around 100°C, the fast pyrolysis of hemicellulose and cellulose with narrow peaks, and the slower pyrolysis of lignins with a wide peak. They overlap because pyrolysis of wood components occurs simultaneously in a narrow temperature range. This hinders the parameter identification through optimization.
The kinetic parameters recovered are provided in **Table 3**. Despite the previously mentioned points, the activation energies match the ones found in literature (see part 3.5).

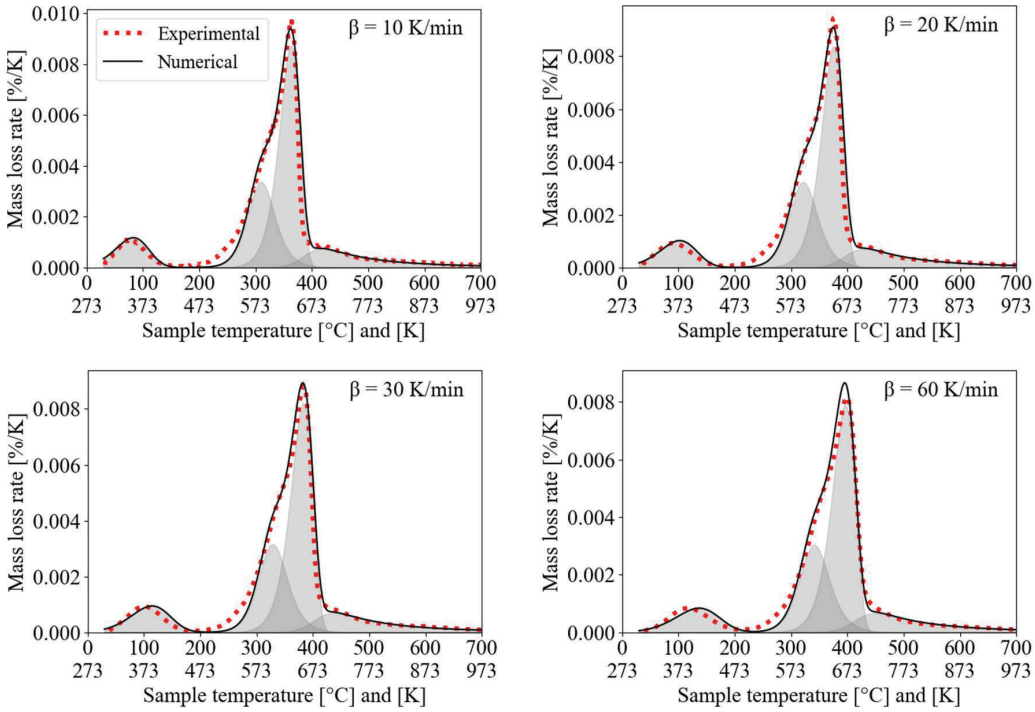

Figure 2: Experimental data (red dotted) and numerical fit (black) by FiTGA. Grey areas represent contribution for each pseudo component reaction

https://doi.org/10.52202/077185-0175

Table 3: Arrhenius parameters for four parallel reaction mechanism

	Water	Hemicellulose	Cellulose	Lignins
Ea [kJ/mol]	34.09	160.71	179.75	226.38
log(A) [s^{-1}]	2.72	12.35	12.71	14.95
F (%)	8.16	21.68	42.03	12.22
n [-]	1.06	1.89	1.00	7.32

From **Table 3**, it is possible to notice that Ea pseudo-hemicellulose < Ea pseudo-cellulose < Ea pseudo-lignins. Keeping in mind that Ea is the minimum energy required to start a reaction, the lower pseudo-hemicellulose Ea value means that this component degrades easier than the two others. The high Ea values associated with pseudo-lignins could be related to its aromatic nature and the fact that this component is the cementing agent of biomass fibers (Mumbach et al. 2022).

3.3 Deconvolution and Isoconversional analysis

Deconvolution of the experimental data using asymmetric gaussians was performed, trying to match the peaks obtained by FiTGA. Parameters such as width, position, tilt and area were modified to obtain sensitive results. **Figure 3** represents the fit of experimental data with four asymmetric gaussian functions, representing the contribution of the four previously cited pseudo-components.
The pseudo components were then regrouped by type in order to get four graphs with four heating rate each, and isoconversional methods were used on each graph. **Figure 4** is an example of the approach with Friedman method: the left-hand side of the Friedman equation is plotted versus -1000/RT (so the resulting slope (Ea) can be in kJ/mol) in each graph, and a linear regression is done for different conversions values (0.05 to 0.95). The resulting slop gives Ea in function of the conversion rate.

The obtained values being quite constant in regard to the conversion rate, only the average values are being looked at. Average values of Energy activation and R^2, as well as pre-exponential factor are given in **Table 4**.

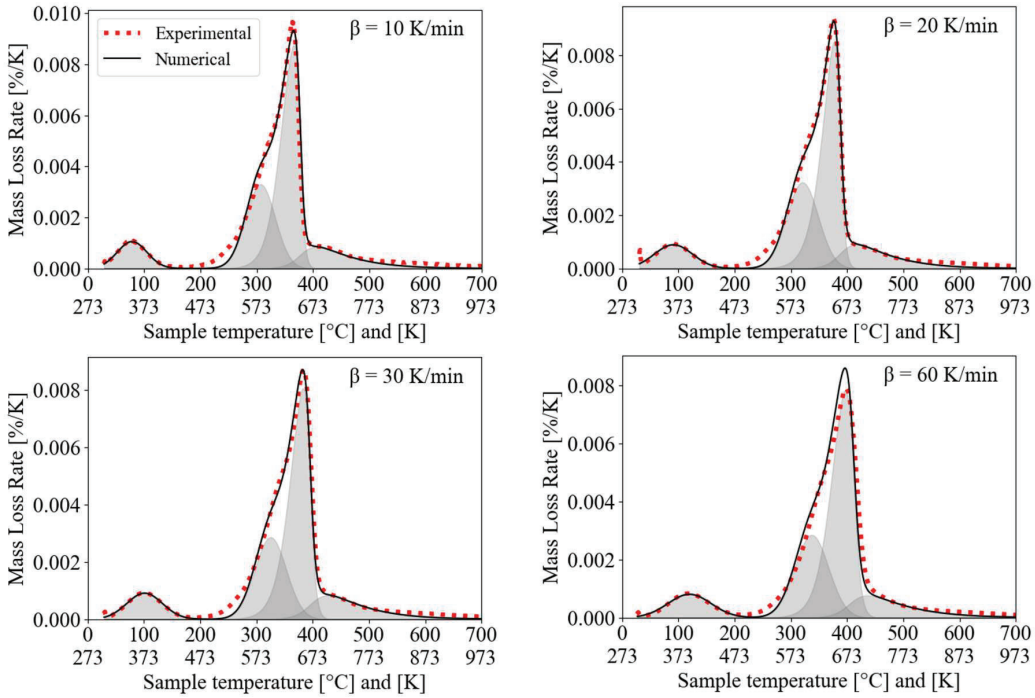

Figure 3: Experimental data (red dotted) and Asym2sig deconvolution (black). Grey areas represent contribution for each pseudo component reaction

https://doi.org/10.52202/077185-0175

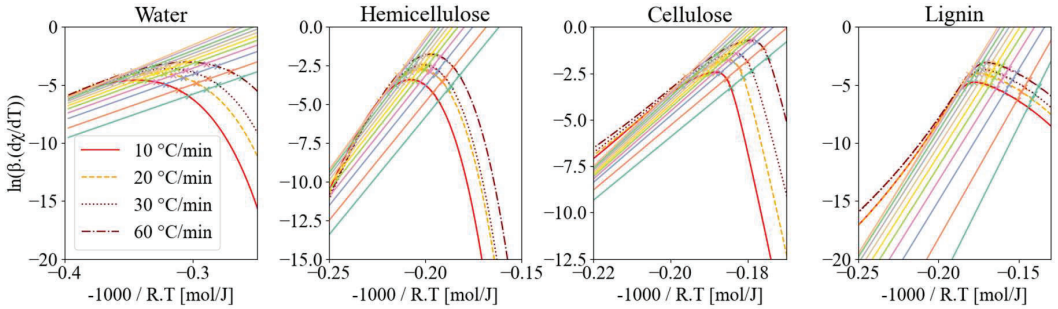

Figure 4: Friedman isoconversional plot at different conversion values [0.05-0.95]

The Ea results obtained with the optimization method, and the three isoconversional methods are in the same order of magnitude. Water activation energy varies from around 10 kJ/mol, hemicellulose one from less than 7 kJ/mol, cellulose one from around 3 kJ/mol and lignins one from less than 2 kJ/mol. Values of $\log(A)$ vary more, especially in the case of water and lignins, but also stays in the same order of magnitude. R^2 average values are satisfactory, with every value being over 98.8%
These results will then be compared with literature in part 3.5.

Table 4: Ea, A and R^2 found with the optimization method FiTGA and with Friedman, Kissinger and OFW isoconversional methods (average values for Ea and R^2)

	Water			Hemicellulose			Cellulose			Lignins		
	Ea [kJ/mol]	log(A) [-]	R² [-]	Ea [kJ/mol]	log(A) [-]	R² [-]	Ea [kJ/mol]	log(A) [-]	R² [-]	Ea [kJ/mol]	log(A) [-]	R² [-]
FiTGA	34.10	2.72		160.71	12.35		179.74	12.71		226.38	14.95	
Friedman	41.25	5.72	0.988	159.85	13.77	0.997	176.84	13.16	0.997	227.38	18.36	0.993
Kissinger	41.58	5.76	0.990	166.32	14.22	0.995	178.20	13.82	0.997	227.96	17.9	0.997
OFW	45.51	6.43	0.992	167.49	14.39	0.995	179.55	13.98	0.997	228.24	18.02	0.997

3.4 DSC analysis

The Heat flow emitted during the pyrolysis process was studied as a function of temperature and heating rate. DSC graphs are plotted in **Figure 5** for the four heating rates studied. Similarly to the TGA curves, the reactions shift toward higher temperatures when the heating rate increases. A first endothermic peak can be seen for water evaporation, then a second before 400°C, immediately followed by a long exothermic one. These two peaks can be identified as the heat flow emitted during the cellulose and lignins decomposition, and confirm the previous positioning of the lignins DTG peak: around the end of the cellulose one, and with an elongated shape. Previous work conducted on pure pseudo-components confirmed this placement (S. Zhang, Mei, and Lin 2024).

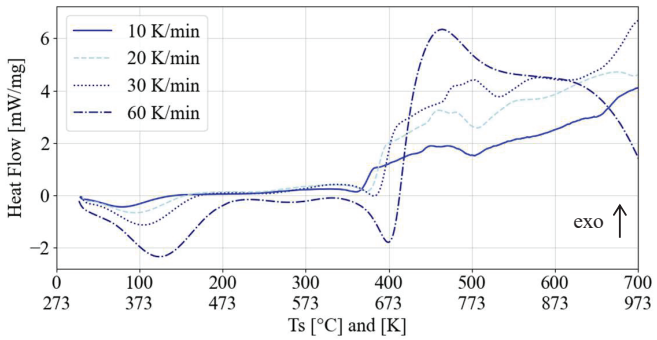

Figure 5: Heat Flow measurement results at different heating rates

https://doi.org/10.52202/077185-0175

3.5 Literature review and comparison

A review has been done on seventeen articles in order to compare the $Ea/\log(A)$ couples in the literature. Selected papers utilized a multi-component model to obtain said couple for water, hemicellulose, cellulose and/or lignins, through optimization or isoconversional methods. They were mainly performed on hard and soft wood samples, but results from other lignocellulosic biomass were also used, as studies proved that the composition and kinetic parameters are comparable (Díez et al. 2020; Wang et al. 2015).

Figure 6 represents the $Ea/\log(A)$ couples found in the literature as well as the distribution of the values Ea (on top) and $\log(A)$ (on the right) found for each pseudo-component. The method and type of biomass used are also distinguished by the shape and the contour of the points. The points can be attributed to the corresponding study through the number written inside following **Table 5**.

Table 5: Literature used in the review

0	This study	6	(Gašparovič et al. 2012)	12	(Janković et al. 2018)
1	(Grønli, Várhegyi, and Di Blasi 2002)	7	(Cai et al. 2013)	13	(Da Silva et al. 2020)
2	(Manyà, Velo, and Puigjaner 2003)	8	(Janković 2014)	14	(Díez et al. 2020)
3	(Sánchez-Jiménez et al. 2011)	9	(J. Zhang et al. 2014)	15	(Torres-Herrador et al. 2020)
4	(Várhegyi et al. 2011)	10	(Wang et al. 2015)	16	(G. Zhang et al. 2022)
5	(Amutio et al. 2012)	11	(Thanatawee et al. 2016)	17	(Rojas et al. 2023)

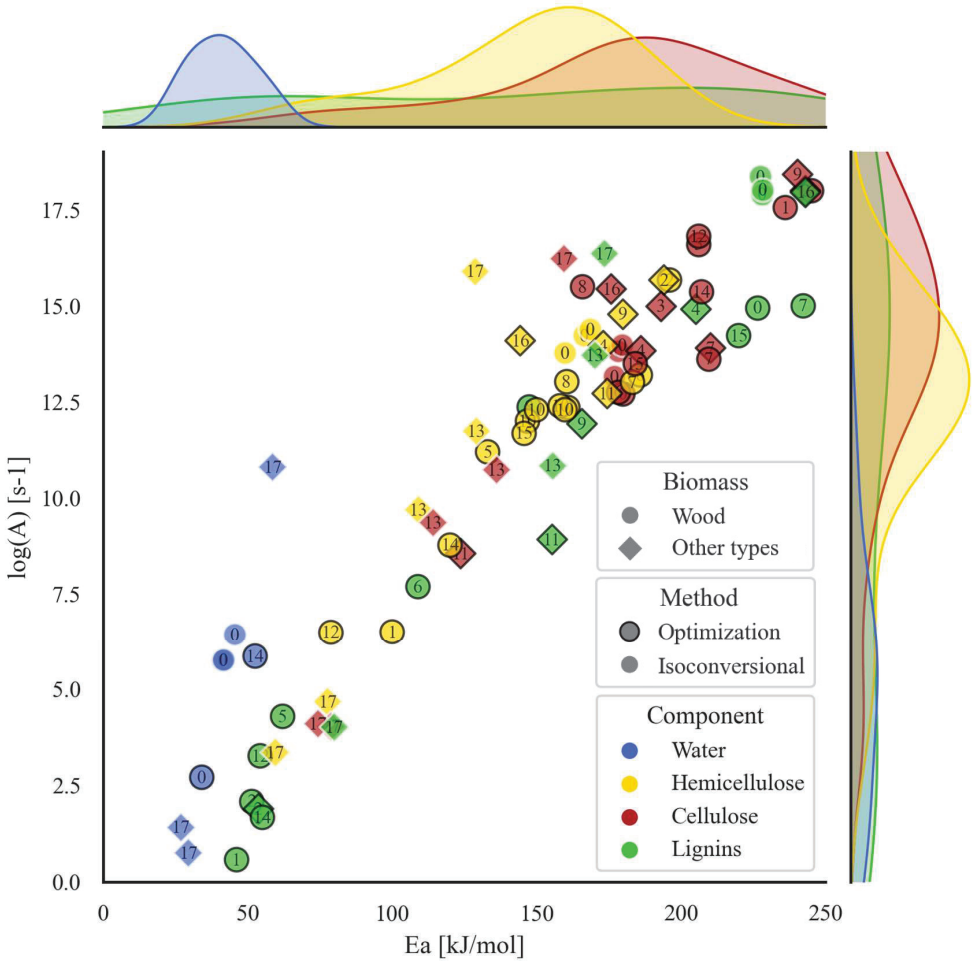

Figure 6: Review of $Ea/\log(A)$ values in literature for wood samples and other lignocellulosic biomass depending on the method and the pseudo-component

https://doi.org/10.52202/077185-0175

The type of wood or type of method used doesn't seem to have too much of an impact on the results, as the different points are distributed equally regarding those criteria. The points seem to follow a linear tendency, with a high Energy activation correlated to a high pre-exponential factor.

The density peaks of Ea values for water, hemicellulose and cellulose are quite narrow, which means that the values don't vary to much in the literature. The observed ranges are 25-60 kJ/mol, 120-200 kJ/mol and 150-250 kJ/mol for those three compounds respectively.
Same goes for $\log(A)$ values of hemicellulose and cellulose, which range between 12-18 s^{-1} and 10-16 s^{-1} respectively. The $\log(A)$ value of water is more distributed, but seems to stay in the lower values.

The real point of contention comes when looking at the lignins. Literature seems to not be able to come to an agreement regarding the kinetic values. This can be explained by the initial evaluation of the lignins decomposition. Indeed, articles in which the values are on the lower side tend to represent lignins decomposition as a very low and large peak, happening throughout the whole range of temperature. On the other hand, results are higher when the decomposition is said to happen at the end of the reaction. Higher values might be more sensible in regard to the chemical complexity of lignins requiring more energy to break and decompose its long carbon chains (Collard and Blin 2014; Mumbach et al. 2022). Moreover, studies performed on pure lignin tend to point towards a decomposition in the higher temperature zones (Thanatawee et al. 2016; S. Zhang, Mei, and Lin 2024)

This paper results are in the interval set by the literature for Water, Hemicellulose and Cellulose pseudo-components. The values found for lignins are in the higher ranges, especially for the isoconversional methods, but still stay comparable to other studies.

4 CONCLUSIONS

This research investigated the kinetic parameters of hardwood biomass during pyrolysis, and the impact of the identification method. It also compared literature studies performed on different types of wood with different methods, in order to highlight the impact of said factors.
The two main method used (in this work and in the literature) are optimization approaches, during which combinations of kinetic factors are optimized until convergence, and isoconversional methods that rely on analytical models.

Activation energies were determined for drying (30-35 kJ/mol), and for the pyrolysis of pseudo components hemicellulose (155-160 kJ/mol), cellulose (170-185 kJ/mol) and lignins (220-230 kJ/mol) with the two methods. The order of activation energy values (Ea) reveals their relative ease of degradation. Pseudo-hemicellulose's lower Ea suggests easier degradation, while pseudo-lignins' higher values align with its aromatic nature and role as the biomass cementing agent. Consistency in Ea results between methods reaffirms their reliability, with $\log(A)$ variations staying within comparable ranges.
DSC measurements allowed to confirm the positioning of pseudo-lignins decomposition peak in regard to the temperature, and also confirmed its exothermic degradation, as showcased by (Di Blasi 2008).

Despite minor influence from wood type or method, distribution peaks of Ea values in literature for pseudo components water, hemicellulose, and cellulose showcase reliable consensus. Lignins however, present a contentious point due to inconsistent kinetic values in the literature. This study's higher values align with lignin's chemical complexity, demanding more energy for decomposition.
This research advances our understanding of hardwood biomass pyrolysis kinetics, emphasizing the need for standardized methodologies and consistent representations in future lignin-related studies.

To conclude, kinetic parameters of hardwood biomass pyrolysis have been found and validated by the literature, allowing to provide data to feed physical simulation model for optimizing pyrolysis processes.

https://doi.org/10.52202/077185-0175

NOMENCLATURE

A	Pre-exponential factor	(s^{-1})
β	Heating rate	($K.min^{-1}$)
χ	Reaction advancement	(-)
Ea	Activation energy	($kJ.mol^{-1}$)
F	Mass loss fraction	
m	Weight	(kg)
n	Reaction order	(-)
OFW	Ozawa-Flynn-Wall	
T	Temperature	(K)
R	Universal Gas Constant	($J.mol^{-1}.K^{-1}$)
R^2	Correlation coefficient	(-)

Subscript

0	Initial
f	Final
p	Peak

REFERENCES

Amutio, Maider, Gartzen Lopez, Roberto Aguado, Maite Artetxe, Javier Bilbao, and Martin Olazar. 2012. "Kinetic Study of Lignocellulosic Biomass Oxidative Pyrolysis." *Fuel* 95: 305–11. doi:10.1016/j.fuel.2011.10.008.

ASTM D 698. 1999. "Test Methods for Arrhenius Kinetics Constants for Thermally Unstable Materials."

Bandara, Janitha C., Rajan Jaiswal, Henrik K. Nielsen, Britt M.E. Moldestad, and Marianne S. Eikeland. 2021. "Air Gasification of Wood Chips, Wood Pellets and Grass Pellets in a Bubbling Fluidized Bed Reactor." *Energy* 233: 121149. doi:10.1016/j.energy.2021.121149.

Blondeau, Julien, and Hervé Jeanmart. 2012. "Biomass Pyrolysis at High Temperatures: Prediction of Gaseous Species Yields from an Anisotropic Particle." *Biomass and Bioenergy* 41: 107–21.

Cai, Junmeng, Weixuan Wu, Ronghou Liu, and George W. Huber. 2013. "A Distributed Activation Energy Model for the Pyrolysis of Lignocellulosic Biomass." *Green Chemistry* 15(5): 1331. doi:10.1039/c3gc36958g.

Chen, Chuihan, Wei Miao, Cheng Zhou, and Hongjuan Wu. 2017. "Thermogravimetric Pyrolysis Kinetics of Bamboo Waste via Asymmetric Double Sigmoidal (Asym2sig) Function Deconvolution." *Bioresource Technology* 225: 48–57. doi:10.1016/j.biortech.2016.11.013.

Collard, François-Xavier, and Joël Blin. 2014. "A Review on Pyrolysis of Biomass Constituents: Mechanisms and Composition of the Products Obtained from the Conversion of Cellulose, Hemicelluloses and Lignin." *Renewable and Sustainable Energy Reviews* 38: 594–608. doi:10.1016/j.rser.2014.06.013.

Corbetta, Michele, Alessio Frassoldati, Hayat Bennadji, Krystle Smith, Michelle J. Serapiglia, Guillaume Gauthier, Thierry Melkior, Eliseo Ranzi, and Elizabeth M. Fisher. 2014. "Pyrolysis of Centimeter-Scale Woody Biomass Particles: Kinetic Modeling and Experimental Validation." *Energy & Fuels* 28(6): 3884–98. doi:10.1021/ef500525v.

Da Silva, Jean Constantino Gomes, Jaqueline Gondim De Albuquerque, Wendell Venicio De Araujo Galdino, Rennio Felix De Sena, and Silvia Layara Floriani Andersen. 2020. "Single-Step and Multi-Step Thermokinetic Study – Deconvolution Method as a Simple Pathway for Describe Properly the Biomass Pyrolysis for Energy Conversion." *Energy Conversion and Management* 209: 112653. doi:10.1016/j.enconman.2020.112653.

Dhaundiyal, Alok, Abdulrahman Th Mohammad, and Toth Laszlo. 2019. "Thermo-Kinetics of Forest Waste Using Model-Free Methods." *Universitas Scientiarum* 24(1): 1–31. doi:10.11144/Javeriana.SC24-1.tofw.

https://doi.org/10.52202/077185-0175

Di Blasi, Colomba. 2008. "Modeling Chemical and Physical Processes of Wood and Biomass Pyrolysis." *Progress in Energy and Combustion Science* 34(1): 47–90. doi:10.1016/j.pecs.2006.12.001.

Díez, David, Ana Urueña, Raúl Piñero, Aitor Barrio, and Tarja Tamminen. 2020. "Determination of Hemicellulose, Cellulose, and Lignin Content in Different Types of Biomasses by Thermogravimetric Analysis and Pseudocomponent Kinetic Model (TGA-PKM Method)." *Processes* 8(9): 1048. doi:10.3390/pr8091048.

Gašparovič, L, J Labovský, and J Markoš. 2012. "Calculation of Kinetic Parameters of the Thermal Decomposition of Wood by Distributed Activation Energy Model (DAEM)." *Chem. Biochem. Eng. Q.*

Grønli, Morten Gunnar, Gábor Várhegyi, and Colomba Di Blasi. 2002. "Thermogravimetric Analysis and Devolatilization Kinetics of Wood." *Industrial & Engineering Chemistry Research* 41(17): 4201–8. doi:10.1021/ie0201157.

Hu, Xun, and Mortaza Gholizadeh. 2019. "Biomass Pyrolysis: A Review of the Process Development and Challenges from Initial Researches up to the Commercialisation Stage." *Journal of Energy Chemistry* 39: 109–43. doi:10.1016/j.jechem.2019.01.024.

Janković, Bojan. 2014. "The Pyrolysis Process of Wood Biomass Samples under Isothermal Experimental Conditions—Energy Density Considerations: Application of the Distributed Apparent Activation Energy Model with a Mixture of Distribution Functions." *Cellulose* 21(4): 2285–2314. doi:10.1007/s10570-014-0263-x.

Janković, Bojan, Nebojša Manić, Dragoslava Stojiljković, and Vladimir Jovanović. 2018. "TSA-MS Characterization and Kinetic Study of the Pyrolysis Process of Various Types of Biomass Based on the Gaussian Multi-Peak Fitting and Peak-to-Peak Approaches." *Fuel* 234: 447–63. doi:10.1016/j.fuel.2018.07.051.

Manyà, Joan J., Enrique Velo, and Luis Puigjaner. 2003. "Kinetics of Biomass Pyrolysis: A Reformulated Three-Parallel-Reactions Model." *Industrial & Engineering Chemistry Research* 42(3): 434–41. doi:10.1021/ie020218p.

Mishra, Ranjeet Kumar, and Kaustubha Mohanty. 2018. "Pyrolysis Kinetics and Thermal Behavior of Waste Sawdust Biomass Using Thermogravimetric Analysis." *Bioresource Technology* 251: 63–74. doi:10.1016/j.biortech.2017.12.029.

Mumbach, Guilherme Davi, José Luiz Francisco Alves, Jean Constantino Gomes Da Silva, Michele Di Domenico, Santiago Arias, Jose Geraldo A. Pacheco, Cintia Marangoni, Ricardo Antonio Francisco Machado, and Ariovaldo Bolzan. 2022. "Prospecting Pecan Nutshell Pyrolysis as a Source of Bioenergy and Bio-Based Chemicals Using Multicomponent Kinetic Modeling, Thermodynamic Parameters Estimation, and Py-GC/MS Analysis." *Renewable and Sustainable Energy Reviews* 153: 111753. doi:10.1016/j.rser.2021.111753.

Park, Won Chan, Arvind Atreya, and Howard R. Baum. 2010. "Experimental and Theoretical Investigation of Heat and Mass Transfer Processes during Wood Pyrolysis." *Combustion and Flame* 157(3): 481–94. doi:10.1016/j.combustflame.2009.10.006.

Ranzi, Eliseo, Alberto Cuoci, Tiziano Faravelli, Alessio Frassoldati, Gabriele Migliavacca, Sauro Pierucci, and Samuele Sommariva. 2008. "Chemical Kinetics of Biomass Pyrolysis." *Energy & Fuels* 22(6): 4292–4300. doi:10.1021/ef800551t.

Rojas, Myriam, Diana Ruano, Estefania Orrego-Restrepo, and Farid Chejne. 2023. "Non-Isothermal Kinetics of Cellulose, Hemicellulose, and Lignin Degradation during Cocoa Bean Shell Pyrolysis." *Biomass and Bioenergy* 177: 106932. doi:10.1016/j.biombioe.2023.106932.

Romero Millán, Lina María, Fabio Emiro Sierra Vargas, and Ange Nzihou. 2017. "Kinetic Analysis of Tropical Lignocellulosic Agrowaste Pyrolysis." *BioEnergy Research* 10(3): 832–45. doi:10.1007/s12155-017-9844-5.

https://doi.org/10.52202/077185-0175

Saeed, M. Azam, M. Farooq, Gordon E. Andrews, Herodotos N. Phylaktou, and Bernard M. Gibbs. 2019. "Ignition Sensitivity of Different Compositional Wood Pellets and Particle Size Dependence." *Journal of Environmental Management* 232: 789–95. doi:10.1016/j.jenvman.2018.11.122.

Sánchez-Jiménez, Pedro E., Luis A. Pérez-Maqueda, Antonio Perejón, José Pascual-Cosp, Mónica Benítez-Guerrero, and José M. Criado. 2011. "An Improved Model for the Kinetic Description of the Thermal Degradation of Cellulose." *Cellulose* 18(6): 1487–98. doi:10.1007/s10570-011-9602-3.

Shafizadeh, Fred, and Peter P. S. Chin. 1977. "Thermal Deterioration of Wood." *Wood Technology: Chemical Aspects*: 57–81. doi:https://doi. org/10/cx27mm.

Sun, Ye, and Jiayang Cheng. 2002. "Hydrolysis of Lignocellulosic Materials for Ethanol Production: A Review q." *Bioresource Technology*.

Thanatawee, Phattharanid, Wanwisa Rukthong, Sasithorn Sunphorka, Pornpote Piumsomboon, and Benjapon Chalermsinsuwan. 2016. "Effect of Biomass Compositions on Combustion Kinetic Parameters Using Response Surface Methodology." *International Journal of Chemical Reactor Engineering* 14(1): 517–26. doi:10.1515/ijcre-2015-0082.

Torres-Herrador, F., V. Leroy, B. Helber, L. Contat-Rodrigo, J. Lachaud, and T. Magin. 2020. "Multicomponent Pyrolysis Model for Thermogravimetric Analysis of Phenolic Ablators and Lignocellulosic Biomass." *AIAA Journal* 58(9): 4081–89. doi:10.2514/1.J059423.

Várhegyi, Gábor, Balázs Bobály, Emma Jakab, and Honggang Chen. 2011. "Thermogravimetric Study of Biomass Pyrolysis Kinetics. A Distributed Activation Energy Model with Prediction Tests." *Energy & Fuels* 25(1): 24–32. doi:10.1021/ef101079r.

Wang, Shurong, Bin Ru, Haizhou Lin, and Wuxing Sun. 2015. "Pyrolysis Behaviors of Four O-Acetyl-Preserved Hemicelluloses Isolated from Hardwoods and Softwoods." *Fuel* 150: 243–51. doi:10.1016/j.fuel.2015.02.045.

Xu, Yiliang, and Baoliang Chen. 2013. "Investigation of Thermodynamic Parameters in the Pyrolysis Conversion of Biomass and Manure to Biochars Using Thermogravimetric Analysis." *Bioresource Technology* 146: 485–93. doi:10.1016/j.biortech.2013.07.086.

Yan, Jingchong, Qitong Yang, Li Zhang, Zhiping Lei, Zhanku Li, Zhicai Wang, Shibiao Ren, Shigang Kang, and Hengfu Shui. 2020. "Investigation of Kinetic and Thermodynamic Parameters of Coal Pyrolysis with Model-Free Fitting Methods." *Carbon Resources Conversion* 3: 173–81. doi:10.1016/j.crcon.2020.11.002.

Zhang, Gang, Qiuyuan Feng, Jinwen Hu, Guang Sun, Fatih Evrendilek, Hui Liu, and Jingyong Liu. 2022. "Performance and Mechanism of Bamboo Residues Pyrolysis: Gas Emissions, by-Products, and Reaction Kinetics." *Science of The Total Environment* 838: 156560. doi:10.1016/j.scitotenv.2022.156560.

Zhang, Jinzhi, Tianju Chen, Jingli Wu, and Jinhu Wu. 2014. "A Novel Gaussian-DAEM-Reaction Model for the Pyrolysis of Cellulose, Hemicellulose and Lignin." *RSC Advances* 4(34): 17513. doi:10.1039/c4ra01445f.

Zhang, Shipeng, Yanyang Mei, and Guiying Lin. 2024. "Pyrolysis Interaction of Cellulose, Hemicellulose and Lignin Studied by TG-DSC-MS." *Journal of the Energy Institute* 112: 101479. doi:10.1016/j.joei.2023.101479.

ACKNOWLEDGEMENT

The authors want to acknowledge M. Francisco Torres-Herrador and his team for the open acces of the FiTGA optimization tool. They would also like to thank Ms. Audrey Duphil and Ms. Cécile Gaborieau for their technical support.

 https://doi.org/10.52202/077185-0175